EDGE ARTICLE

Rate-determining step in the self-assembly process of supramolecular coordination capsules

Yuya Tsujimoto,[a] Tatsuo Kojima[a] and Shuichi Hiraoka[*a]

An in-depth understanding of the self-assembly process at the molecular level is crucial in both biological and materials science fields. However, such research is scarce due to the difficulty in monitoring a great deal of fragmentary species that are transiently produced in the process. We present a novel method for investigating the self-assembly process of supramolecular coordination assemblies by following the time variation of the average composition of the fragmentary species, which was indirectly determined by spectroscopy. With this method, we found that the final stage is the rate-determining step of the self-assembly of an octahedron-shaped coordination capsule, and that the relative energy barrier of each step is controllable by modifying the chemical structure of the building blocks.

Introduction

Supramolecular self-assembly is the process through which molecular building blocks organize themselves to form well-defined structures.[1-5] While the formation of the self-assemblies is often rationalized by their thermodynamic stability, their formation mechanism remains unclear.[6-10] However, in order to properly control the course of self-assembly, an in-depth understanding of the self-assembly process is highly desirable. Supramolecular coordination assemblies are constructed from metal ions and ligand molecules possessing several coordination sites as building blocks. Although a variety of coordination supramolecular assemblies[11-24] and their unique functions[25-33] have been reported in the last two decades, the self-assembly process has scarcely been studied at the molecular level so far.[34-56] This is mainly because it is generally impossible to directly detect the fragmentary species that are transiently produced in the self-assembly process. Herein we report a novel method to investigate the formation mechanism of coordination self-assemblies by monitoring the time variation of the average composition of the fragmentary species, which is indirectly determined by ^{1}H NMR spectroscopy.

[a] Department of Basic Science, Graduate School of Arts and Sciences, The University of Tokyo, 3-8-1 Komaba, Meguro-ku, Tokyo, Japan. E-mail: chiraoka@mail.ecc.u-tokyo.ac.jp

† Electronic Supplementary Information (ESI) available: Experimental Details, additional data, ^{1}H NMR spectra, and ESI-TOF mass spectra. See DOI: 10.1039/b000000x/

Method

Let us consider the formation of a molecular square, $[M_4L_4]^{4m+}$, consisting of four metal ions with a linear coordination geometry, M^{m+}, and four L-shaped organic ligands, L (Fig. 1A). During the formation of $[M_4L_4]^{4m+}$, various fragmentary species should be produced, and are finally converted to the molecular square. To investigate the self-assembly process in a straightforward way, it is necessary to follow the time variation of all the fragmentary species. NMR is superior in view of quantifying and discriminating structurally similar species. However, with some exceptions, it is generally hard to detect the fragmentary species produced in the self-assembly because these fragmentary species have much lower symmetry and because the conversion of the species takes place during measuring the NMR spectrum. We envisaged that it would be possible to obtain the information about the fragmentary species indirectly by quantifying all the species other than the fragmentary species. In a general coordination self-assembly using M^{m+} as a metal source, while the quantitative analysis of the organic ligand, L, and the molecular square, $[M_4L_4]^{4m+}$, is possible by ^{1}H NMR measurement, that of M^{m+} ions is difficult. By using $[MX_2]^{m+}$ possessing ^{1}H NMR-detectable monodentate ligands, X, instead of M^{m+}, it becomes possible to quantify M^{m+} in the assembly process. In this reaction scheme, the self-assembly proceeds accompanied by the release of X, which can also be detected by ^{1}H NMR. Consequently, all the species other than the fragmentary species, L, $[MX_2]^{m+}$, $[M_4L_4]^{4m+}$ and X, can be quantified in any cases.

Fig. 1 (A) A schematic representation of the self-assembly of a molecular square, $[M_4L_4]^{4m+}$, from metal ion, $[MX_2]^{m+}$ and L-shaped ligands. Since X is NMR-detectable, the average composition of the fragmentary species, $(M_aL_bX_c)_{ave}$, can be monitored by quantifying all of the species other than the fragmentary species, $[MX_2]^{m+}$, L, $[M_4L_4]^{4m+}$ and X. The (n, k) values for several fragmentary species, which are calculated by equations (1) and (2), are shown. (B) A reaction scheme for the assembly of an octahedron-shaped molecular capsule, $[Pd_6L_8]^{12+}$ (L = 1 or 2).

The fragmentary species produced in the self-assembly process consist of L, M^{m+} and X to be expressed as $[M_aL_bX_c]^{ma+}$. To characterize $[M_aL_bX_c]^{ma+}$ more comprehensively, we define two parameters, n and k, as follows:

n is defined as the average number of metal ions binding to a ligand

$$n = (N \cdot a - c)/b \qquad (1)$$

k is defined as metal to ligand ratio

$$k = a/b \qquad (2)$$

where N is a coordination number and in the case of the molecular square $N = 2$. The (n, k) values for $[M_4L_4]^{4m+}$ and several fragmentary species are shown in Figure 1A. In the experiment, the average composition of the fragmentary species, $(M_aL_bX_c)_{ave}$, can be monitored by quantifying L, $[MX_2]^{m+}$, $[M_4L_4]^{4m+}$ and X. As a result, we can investigate the self-assembly process from the time evolution of the (n, k) value for $(M_aL_bX_c)_{ave}$.

In this report, employing this method, we investigated the self-assembly process of an octahedron-shaped molecular capsule, $[Pd_6L_8]^{12+}$, constructed from triangle-shaped panel molecules L (L = 1 or 2) and $[PdPy_4]^{2+}$ (Py stands for pyridine) (Fig. 1B). The formation of $[Pd_61_8]^{12+}$ from 1 and $[Pd(CH_3CN)_4]^{2+}$ was previously demonstrated by NMR and electrospray ionization (ESI) mass measurements.[24] The single crystal X-ray analysis of its isostructure, $[Hg_61_8]^{12+}$, revealed an octahedron-shaped capsule structure. Since Pd^{2+} ion has a square-planar coordination geometry, $N = 4$. In this case, both n and k range from 0 to 3. As a particular case, the (n, k) value of the molecular capsule, $[Pd_6L_8]^{12+}$, is (3.00, 0.75). We counted all of the possible fragmentary species with different compositions, $[Pd_aL_bPy_c]^{2a+}$ ($a \leq 6$, $b \leq 8$), smaller than $[Pd_6L_8]^{12+}$ (154 species). The (n, k) values for these fragmentary species and the molecular capsule are plotted to obtain an n-k map for the assembly of the molecular capsule, $[Pd_6L_8]^{12+}$ (Figs 2A and S1†). Thus one can investigate the self-assembly process by monitoring the time variation of the (n, k) value for the average composition of the fragmentary species.
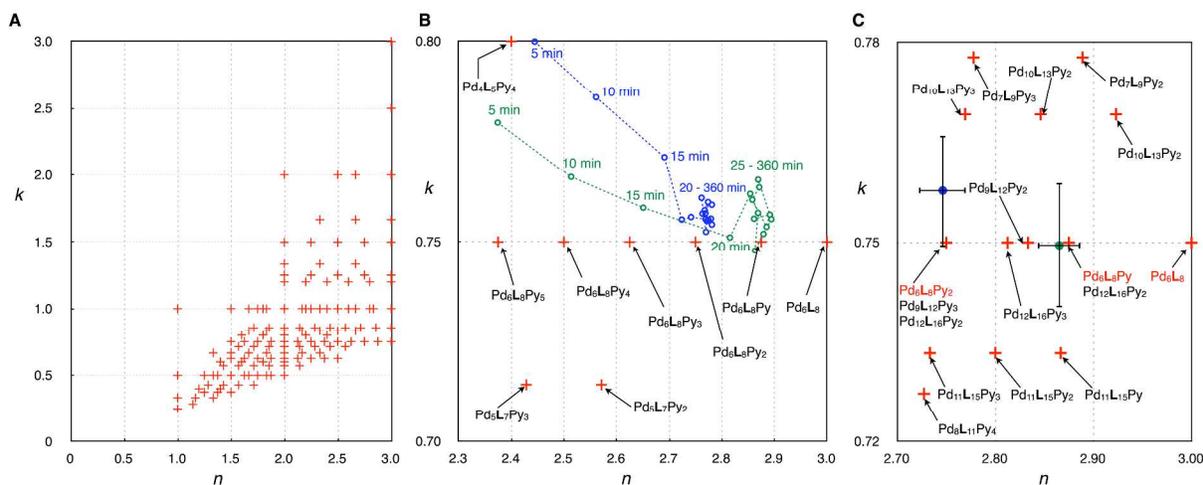
Fig. 2 (A) An n-k map for the assembly of $[Pd_6L_8]^{12+}$. Red crosshairs denote the (n, k) values of 154 possible fragmentary species and the capsule. (B) The time variation of the (n, k) value for the average composition of the fragmentary species, $(Pd_aL_bPy_c)_{ave}$, during the self-assembly of $[Pd_61_8]^{12+}$ (green open circles) and $[Pd_62_8]^{12+}$ (blue open circles) on the n-k map. (C) Partial n-k map for the species $Pd_aL_bPy_c$ ($1 \leq a \leq 12$, $1 \leq b \leq 16$). Red crosshairs indicate the (n, k) values of $Pd_aL_bPy_c$ ($1 \leq a \leq 12$, $1 \leq b \leq 16$). The average (n, k) values obtained from 20 to 360 min for the assembly of $[Pd_61_8]^{12+}$ and $[Pd_62_8]^{12+}$ are plotted as filled green and blue circles, respectively.

Results and discussion

In the presence of 1,3,5-trimethoxybenzene as an internal standard, the formation of $[Pd_6\mathbf{1}_8]^{12+}$ from $\mathbf{1}$ and $[PdPy_4]^{2+}$ was monitored by ^1H NMR measurement at 298 K with a 5-minute interval.[57] Several ^1H NMR spectra are shown in Fig. 3A. $[Pd_6\mathbf{1}_8]^{12+}$ is preferentially formed from $\mathbf{1}$ and $[PdPy_4]^{2+}$ over 80% yield after 6 hours (Fig. 5D). From enthalpic point of view, the capsule formation does not seem preferable so much because the strength of Pd–N coordination bonding in the starting $[PdPy_4]^{2+}$ is comparable to that in the molecular capsule $[Pd_6\mathbf{1}_8]^{12+}$. On the other hand, the capsule formation is entropically favourable due to the release of 24 Py molecules. According to these considerations, the formation of the molecular capsule would be driven by an entropic factor. It is noteworthy that since this entropic effect would always prefer the formation of coordination assemblies, this method is widely applicable to other coordination assemblies.

The average composition of the fragmentary species, $(Pd_a\mathbf{L}_b Py_c)_{ave}$, was calculated by ^1H NMR signals for $\mathbf{1}$, $[Pd_6\mathbf{1}_8]^{12+}$, $[PdPy_4]^{2+}$ and Py (Tables S2-S11†). Thus the (n, k) values for $(Pd_a\mathbf{L}_b Py_c)_{ave}$ at each time were obtained using equations (1) and (2), and were plotted on the n-k map (Fig. 2B and Tables S2-S11†). The (n, k) value measured after 5 min showed $(2.37, 0.78)$ and as times passed, n increased but k slightly decreased. Finally the (n, k) value reached $(2.85, 0.76)$ at 25 min and stayed until 360 min. This behaviour was reproducible and the average (n, k) value from $(n, k)_{25\,min}$ to $(n, k)_{360\,min}$ obtained from ten repetitive measurements was found to be $(2.87 \pm 0.02, 0.75 \pm 0.01)$ (Fig. 2C). To simplify the discussion, we assume that the capsule is formed from fragmentary species $\mathbf{A}$ (n_A, k_A) via fragmentary species $\mathbf{B}$ (n_B, k_B). If the conversion from $\mathbf{B}$ to the capsule is slower than that from $\mathbf{A}$ to $\mathbf{B}$, the composition of $\mathbf{B}$ in the fragmentary species increases gradually and thus the (n, k) value of the fragmentary species becomes close to (n_B, k_B). Finally all $\mathbf{A}$ converts to $\mathbf{B}$, at which time the (n, k) value reaches (n_B, k_B). After that time, although the self-assembly proceeds by the conversion of $\mathbf{B}$ to the capsule, the (n, k) value stays at (n_B, k_B). In this example, the step from $\mathbf{B}$ to the capsule is the rate-determining step of the self-assembly. From 25 to 360 min, during which the formation of the molecular capsule proceeds, the (n, k) value of the fragmentary species remained unchanged (Fig. 2B). On the basis of the above discussion, the dominant fragmentary species after 25 min should be $[Pd_6\mathbf{1}_8 Py_1]^{12+}$, whose (n, k) value is the closest to the average (n, k) value found by experiment, $(2.87 \pm 0.02, 0.75 \pm 0.01)$, and the final step of the self-assembly from $[Pd_6\mathbf{1}_8 Py_1]^{12+}$ to $[Pd_6\mathbf{1}_8]^{12+}$ should be the rate-determining step.[58]

The existence of $[Pd_6\mathbf{1}_8 Py_1]^{12+}$ with a proper lifetime in the self-assembly process was unambiguously demonstrated by ESI mass spectrometry. Although at the initial stage of the self-assembly (within 15 min) any signals for the $[Pd_6\mathbf{1}_8 Py_1]^{12+}$ complex were not found, the signals assignable to $[Pd_6\mathbf{1}_8 Py_1(CF_3SO_3)_m]^{(12-m)+}$ ($m = 5, 6, 7, 8$) appeared after 20 min (Fig. S4†).
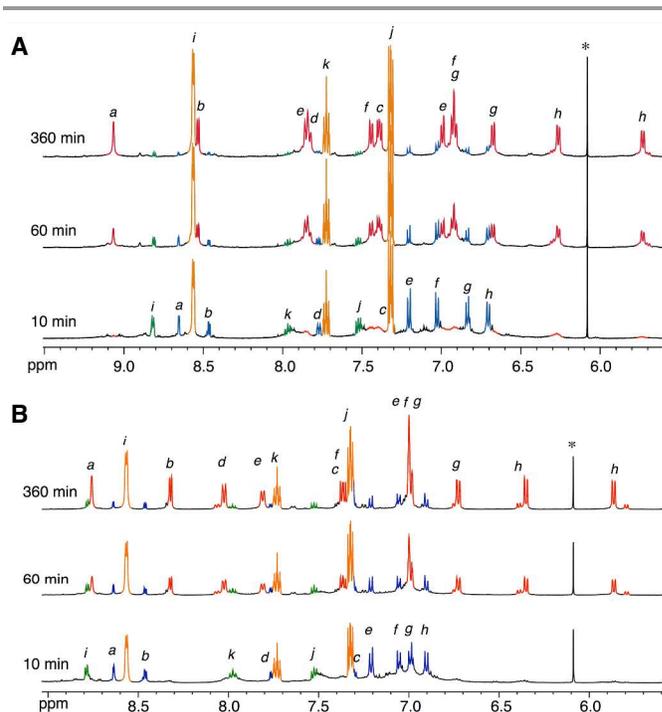
Fig. 3 ^1H NMR spectra (500 MHz, CD$_3$CN:CD$_2$Cl$_2$ (v/v = 3.6:1, 298 K). Formation of $[Pd_6\mathbf{1}_8]^{12+}$ from $\mathbf{1}$ and PdPy$_4$·(OTf)$_2$ (A) and formation of $[Pd_6\mathbf{2}_8]^{12+}$ from $\mathbf{2}$ and PdPy$_4$·(OTf)$_2$ (B). The signals colored in red, green, blue and orange indicate $[Pd_6\mathbf{L}_8]^{12+}$, $[PdPy_4]^{2+}$, $\mathbf{L}$ and Py, respectively. Asterisk indicates one of ^1H signals for 1,3,5-trimethoxybenzene which was used as an internal standard.

In the self-assembly process of the $[Pd_6\mathbf{L}_8]^{12+}$ capsule, the formation of species larger than the molecular capsule, $[Pd_x\mathbf{L}_y Py_z]^{2x+}$ ($x > 6$ and/or $y > 8$), might be possible. However, even in the consideration of the formation of $[Pd_x\mathbf{L}_y Py_z]^{2x+}$ ($1 \leq x \leq 12$, $1 \leq y \leq 16$), the most appropriate species whose (n, k) value is the closest to the average (n, k) value found by experiment are $[Pd_6\mathbf{L}_8 Py_1]^{12+}$ and its dimeric species $[Pd_{12}\mathbf{L}_{16} Py_2]^{24+}$ $(2.88, 0.75)$ (Fig. 2C). If the dimeric $[Pd_{12}\mathbf{L}_{16} Py_2]^{24+}$ is produced in the self-assembly process, the rate-determining step should be the division of $[Pd_{12}\mathbf{L}_{16} Py_2]^{24+}$ triggered by the coordination of two Py molecules, resulting in the formation of two fragmentary species, $[Pd_d\mathbf{L}_e Py_f]^{2d+}$ and $[Pd_{12-d}\mathbf{L}_{16-e} Py_{4-f}]^{(24-2d)+}$. Since the (n, k) values of the two species are invariably different from $(2.88, 0.75)$, both fragmentary species produced by the division of $[Pd_{12}\mathbf{L}_{16} Py_2]^{24+}$ must transform to $[Pd_6\mathbf{L}_8]^{12+}$ quickly to keep the observed (n, k) value unchanged. Although the present data do not definitely exclude the possibility of the dimeric species in the pathway, the process via $[Pd_6\mathbf{L}_8 Py_1]^{12+}$ would be more probable because the formation of $[Pd_6\mathbf{L}_8]^{12+}$ took place smoothly at ambient temperature.

The (n, k) analysis reveals that the final step becomes the rate-determining step of the self-assembly of $[Pd_6\mathbf{1}_8]^{12+}$ even though it is an intramolecular ligand exchange. This finding can be interpreted by considering "associative ligand exchange mechanism" around a square-planar Pd^{2+} centre.[59-61] It is well known that five-coordinate Pd^{2+} centres with square-pyramidal

and trigonal-bipyramidal coordination geometries are intermediately formed during the ligand exchange (Fig. 4A). Since the structure of $[Pd_6\mathbf{1}_8Py_1]^{12+}$ is not completely but almost octahedral, the panel molecules are so closely packed with each other that the motion of the panel molecules would be highly restricted (Fig. 4B). Accordingly, the distorted octahedron-shaped $[Pd_6\mathbf{1}_8Py_1]^{12+}$ structures with one Pd^{2+} centre a five-coordinate geometry, which must be formed during the final step of the self-assembly, should be significantly destabilized, and hence the energy barrier of the step would be increased.
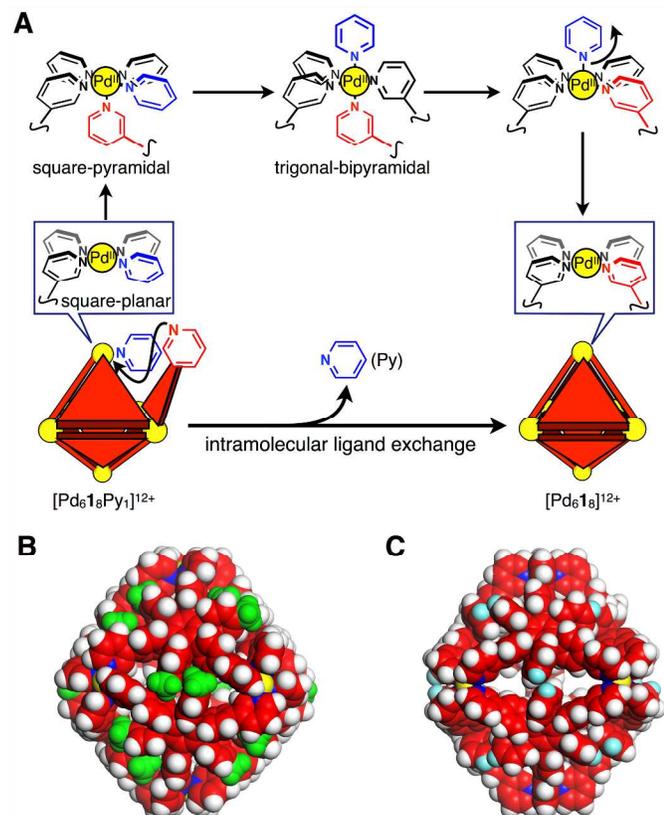
Fig. 4 (A) A plausible reaction mechanism of the intramolecular ligand exchange on a square-planar Pd^{2+} centre in $[Pd_6\mathbf{1}_8Py_1]^{12+}$. (B) and (C) Molecular modeling structures of $[Pd_6\mathbf{1}_8]^{12+}$ (B), and $[Pd_6\mathbf{2}_8]^{12+}$ (C). The structures are constructed based on the crystal structure of their isostructure, $[Hg_6\mathbf{1}_8]^{12+}$. Color labels: red: carbon; white: hydrogen; blue: nitrogen; yellow: palladium; cyan: deuterium; green: methyl group in $[Pd_6\mathbf{1}_8]^{12+}$.

According to the above-mentioned reaction mechanism, modifying the chemical structure of the panel molecule would alter the energy barrier of each step in the self-assembly process. For example, if the three methyl groups of $\mathbf{1}$ are replaced with smaller deuterium atoms,[62] the structural flexibility of $[Pd_6\mathbf{2}_8Py_1]^{12+}$ as well as the capsule, $[Pd_6\mathbf{2}_8]^{12+}$, would become higher due to the decreased interaction between the neighbouring panel molecules (Fig. 4C). Thus, the energy barrier of the final step for the self-assembly of $[Pd_6\mathbf{2}_8]^{12+}$ is expected to be lower than that for $[Pd_6\mathbf{1}_8]^{12+}$. The time variation of the observed (n, k) value of the fragmentary species for the assembly of $[Pd_6\mathbf{2}_8]^{12+}$ is shown in Fig. 2B. The trend is very

similar to the assembly of $[Pd_6\mathbf{1}_8]^{12+}$ but the (n, k) values after 20 min stay around (2.76, 0.76). The average (n, k) value of ten repetitive experiments exhibits (2.75 ± 0.02, 0.76 ± 0.01) (Fig. 2C), indicating that the intramolecular ligand exchange from $[Pd_6\mathbf{2}_8Py_2]^{12+}$ to $[Pd_6\mathbf{2}_8Py_1]^{12+}$ is the rate-determining step.[63] This result indicates that the relative energy barrier of each step in the assembly process depends on the chemical structure of the panel molecule.
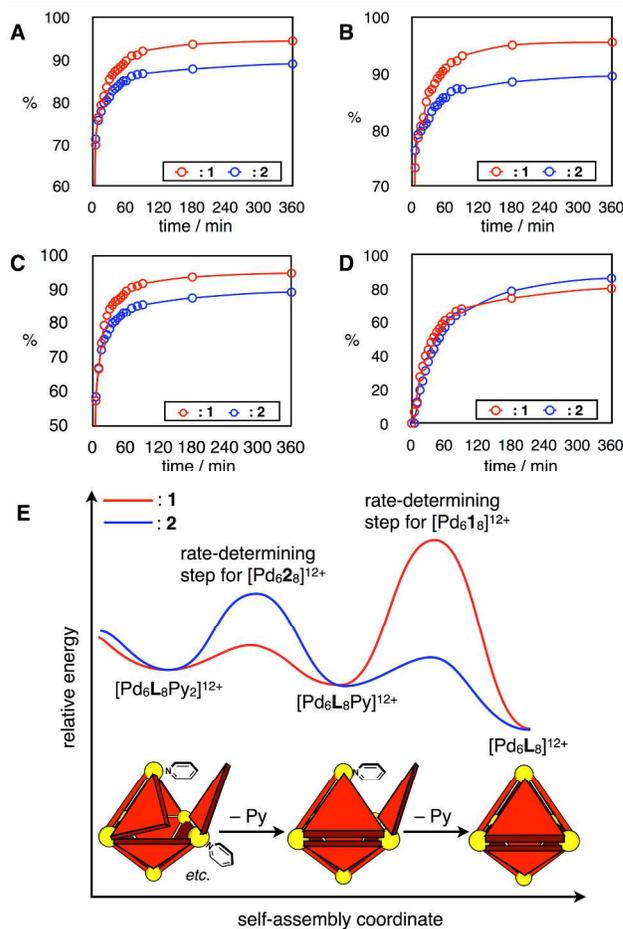
Fig. 5 Effect of the structure of building blocks on the self-assembly. (A) The rates of consumption of ligands, $\mathbf{1}$ in red and $\mathbf{2}$ in blue. (B) The rate of consumption of $[PdPy_4]^{2+}$. (C) The rate of release of Py. (D) The rate of formation of the molecular capsules, $[Pd_6\mathbf{L}_8]^{12+}$ ($\mathbf{L} = \mathbf{1}$ or $\mathbf{2}$). (E) A schematic representation of a potential energy profile for the assembly of the molecular capsules.[63]

It is notable that the rates of consumption of both the panel molecule, $\mathbf{1}$ and $[PdPy_4]^{2+}$ for the self-assembly of $[Pd_6\mathbf{1}_8]^{12+}$ are faster than those for $[Pd_6\mathbf{2}_8]^{12+}$ (Figs 5A and 5B). In addition, the rate of the release of Py for the self-assembly of $[Pd_6\mathbf{1}_8]^{12+}$ is also faster than that for $[Pd_6\mathbf{2}_8]^{12+}$ (Fig. 5C). These results suggest that the rates of the reaction steps before the rate-determining step of the self-assembly of $[Pd_6\mathbf{1}_8]^{12+}$ would be faster than those of $[Pd_6\mathbf{2}_8]^{12+}$. However, the rate of the formation of the molecular capsule is not so different between the two (Fig. 5D). This finding indicates that although the rate of the formation of $[Pd_6\mathbf{1}_8Py_1]^{12+}$ is faster than that of

$[Pd_6\mathbf{2}_8Py_2]^{12+}$, the reaction from $[Pd_6\mathbf{1}_8Py_1]^{12+}$ is much slower than that from $[Pd_6\mathbf{2}_8Py_2]^{12+}$ (Fig. 5E). Consequently, the rates of the formation of $[Pd_6\mathbf{1}_8]^{12+}$ and $[Pd_6\mathbf{2}_8]^{12+}$ become similar to each other. The acceleration of the formation of $[Pd_6\mathbf{1}_8Py_1]^{12+}$ is probably due to the preferential formation of the fragmentary species possessing a partial octahedron-shaped structure arising from the attractive interaction such as van der Waals interaction between the neighbouring panel molecules.[64]

Conclusions

In conclusion, we have developed a novel method for the investigation of the self-assembly process for coordination assemblies by indirectly monitoring the average composition of the fragmentary species that are difficult to characterize and quantify by any spectroscopic techniques. This strategy is widely applicable to the investigation of the assembly process for other discrete coordination assemblies. The self-assembly process is a non-equilibrium system that progresses toward equilibrium or another non-equilibrium state.[65] Our findings indicate that the rate-determining step in the molecular self-assembly is affected by the chemical structure of the ligand molecule and the property of the metal centre as a result of the changes in the energy barrier of each elementary reaction step. This means that on the self-assembly process the modification of building blocks and assembly conditions enables us to deliberately trap a metastable species[66] that exhibits unique functions, as is found in biological systems.[67]

Acknowledgements

Notes and references

1. J. S. Lindsey, *New J. Chem.*, 1991, **15**, 153 – 180.
2. J.-M. Lehn, *Science*, 2002, **295**, 2400 – 2403.
3. G. M. Whitesides, J. P. Mathias and C. T. Seto, *Science*, 1991, **254**, 1312 – 19.
4. D. Philp and J. F. Stoddart, *Angew. Chem., Int. Ed.,* 1996, **35**, 1154 – 1196.
5. A. Klug, *Angew. Chem., Int. Ed.,* 1983, **22**, 565 – 582.
6. G. E. Poirier and E. D. Pylant, *Science*, 1996, **272**, 1145 – 1148.
7. D. K. Schwartz, *Annu. Rev. Phys. Chem.,* 2001, **52**, 107 – 137.
8. S. Mann, *Nat. Mat.,* 2009, **8**, 781 – 792.
9. A. R. Dinner, A. Sali, L. J. Smith, C. M. Dobson and M. Karplus, *Trends Biochem. Sci.,* 2000, **25**, 331 – 339.
10. P. A. P. A. Korevaar, S. J. George, A. J. Markvoort, M. M. J. Smulders, P. A. J. Hilbers, A. P. H. J. Schenning, T. F. A. De Greef and E. W. Meijer, *Nature,* 2012, **481**, 492 – 497.
11. G. F. Swiegers and T. J. Malefetse, *Chem. Rev.,* 2000, **100**, 3483 – 3537.
12. M. Albrecht, *Chem. Rev.,* 2001, **101**, 3457 – 3497.
13. M. Fujita, K. Umemoto, M. Yoshizawa, N. Fujita, T. Kusukawa and K. Biradha, *Chem. Commun.,* 2001, 509 – 518.
14. M. Fujita, M. Tominaga, A. Hori and B. Therrien, *Acc. Chem. Res.,* 2005, **38**, 369 – 378.
15. S. Leininger, B. Olenyuk and P. J. Stang, *Chem. Rev.,* 2000, **100**, 853 – 907.
16. R. Chakrabarty, P. S. Mukherjee and P. J. Stang, *Chem. Rev.,* 2011, **111**, 6810 – 6918.
17. D.-L. Long, E. Burkholder and L. Cronin, *Chem. Soc. Rev.,* 2007, **36**, 105 – 121.
18. P. J. Steel, *Acc. Chem. Res.,* 2005, **38**, 243 – 250.
19. S. J. Dalgarno, N. P. Power and J. L. Atwood, *Coord. Chem. Rev.,* 2008, **252**, 825 – 841.
20. M. J. Zaworotko, *Cryst. Growth Des.,* 2007, **7**, 4 – 9.
21. T. R. Cook, Y.-R. Zheng and P. J. Stang, *Chem. Rev.,* 2013, **113**, 734 – 777.
22. M. T. Pope and A. Müeller, *Angew. Chem., Int. Ed.,* 1991, **30**, 34 – 48.
23. U. Kortz, A. Müller, J. van Slageren, J. Schnack, N. S. Dalal and M. Dressel, *Coord. Chem. Rev.,* 2009, **253**, 2315 – 2327.
24. S. Hiraoka, K. Harano, M. Shiro, Y. Ozawa, N. Yasuda, K. Toriumi and M. Shionoya, *Angew. Chem., Int. Ed.,* 2006, **45**, 6488 – 6491.
25. U. Mueller, M. Schubert, F. Teich, H. Puetter, K. Schierle-Arndt and J. Pastre, *J. Mat. Chem.,* 2006, **16**, 626 – 636.
26. B. Chen, S. Xiang and G. Qian, *Acc. Chem. Res.,* 2010, **43**, 1115 – 1124.
27. G. Aromi and E. K. Brechin, *Struct. Bond.,* 2006, **122**, 1 – 67.
28. M. Yoshizawa, J. K. Klosterman and M. Fujita, *Angew. Chem., Int. Ed.,* 2009, **48**, 3418 – 3438.
29. M. P. Suh, Y. E. Cheon and E. Y. Lee, *Coord. Chem. Rev.,* 2008, **252**, 1007 – 1026.
30. L. R. MacGillivray, G. S. Papaefstathiou, T. Friščić, T. D. Hamilton, D.-K. Bučar, Q. Chu, D. B. Varshney and I. G. Georgiev, *Acc. Chem. Res.,* 2008, **41**, 280 – 291.
31. M. D. Pluth, R. G. Bergman and K. N. Raymond, *Acc. Chem. Res.,* 2009, **42**, 1650 – 1659.
32. C. M. Doherty, D. Buso, A. J. Hill, S. Furukawa, S. Kitagawa and P. Falcaro, *Acc. Chem. Res.,* 2014, **47**, 396 – 405.
33. J.-P. Collin, C. Dietrich-Buchecker, P. Gaviña, M. C. Jimenez-Molero and J.-P. Sauvage, *Acc. Chem. Res.,* 2001, **34**, 477 – 487.
34. A. V. Davis, R. M. Yeh and K. N. Raymond, *Proc. Nat. Acad. Sci. USA,* 2002, **99**, 4793 – 4796.
35. N. Fatin-Rouge, S. Blanc, A. Pfeil, A. Rigault, A.-M. Albrecht-Gray and J.-M. Lehn, *Helv. Chim. Acta,* 2001, **84**, 1694 – 1711.
36. S. Sato, Y. Ishido and M. Fujita, *J. Am. Chem. Soc.,* 2009, **131**, 6064 – 6065.
37. M. D. Levin and P. J. Stang, *J. Am. Chem. Soc.,* 2000, **122**, 7428 – 7429.
38. H. N. Miras, G. J. T. Cooper, D.-T. Long, H. Bögge, A. Müller, C. Streb and L. Cronin, *Science,* 2010, **327**, 72 – 74.
39. J. J. Pak, J. Greaves, D. J. McCord and K. Shea, *Organometallics,* 2002, **21**, 3552 – 3561.

40. Y.-R. Zheng and P. J. Stang, *J. Am. Chem. Soc.,* 2009, **131**, 3487 – 3489.

41. M. Barboiu, G. Vaughan, R. Graff and J.-M. Lehn, *J. Am. Chem. Soc.,* 2003, **125**, 10257 – 10265.

42. E. Leize, A. Van Dorsselaer, R. Krämer and J.-M. Lehn, *J. Chem. Soc., Chem. Commun.,* 1993, 990 – 993.

43. A. Marquis-Rigault, A. Dupont-Gervais, P. N. Baxter, A. Van Dorsselaer and J.-M. Lehn, *Inorg. Chem.,* 1996, **35**, 2307 – 2310.

44. A. Marquis-Rigault, A. Dupont-Gervais, A. Van Dorsselaer and J.-M. Lehn, *Chem. Eur. J.,* 1996, **2**, 1395 – 1398.

45. A. Marquis, J. Kintzinger, R. Graff, P. N. Baxter and J.-M. Lehn, *Angew. Chem., Int. Ed.,* 2002, **41**, 2760 – 2764.

46. C. Su, Y. Cai, C. Chen, F. Lissner, B. Kang and W. Kaim, *Angew. Chem., Int. Ed.,* 2002, **41**, 3371 – 3375.

47. M. Barboiu, E. Petit and G. Vaughan, *Chem. Eur. J.,* 2004, **10**, 2263 – 2270.

48. S. J. Dalgarno, N. P. Power, J. E. Warren and J. L. Atwood, *Chem. Commun.,* 2008, 1539 – 1541.

49. J. Vacek, D. C. Caskey, D. Horinek, R. K. Shoemaker, P. J. Stang and J. Michl, *J. Am. Chem. Soc.,* 2008, **130**, 7629 – 7638.

50. V. M. Cangelosi, T. G. Carter, L. N. Zakharov and D. W. Johnson, *Chem. Commun.,* 2009, 5606 – 5608.

51. T. M. Fyles and C. C. Tong, *New J. Chem.,* 2007, **31**, 296 – 304.

52. C. A. Schalley, T. Müller, P. Linnartz, M. Witt, M. Schäfer and A. Lützen, *Chem. Eur. J.,* 2002, **8**, 3538 – 3551.

53. W. Jiang, A. Schäfer, P. C. Mohr and C. A. Schalley, *J. Am. Chem. Soc.,* 2010, **132**, 2309 – 2320.

54. B. Brusilowskij, S. Neubacher and C. A. Schalley, *Chem. Commun.,* 2009, 785 – 787.

55. M. Yoneya, T. Yamaguchi, S. Sato and M. Fujita, *J. Am. Chem. Soc.,* 2012, **134**, 14401 − 14407.

56. M. Yoneya, S. Tsuzuki, T. Yamaguchi, S. Sato and M. Fujita, *ACS Nano,* 2014, **8**, 1290 – 1296.

57. In most cases, the self-assembly of Pd(II)-linked coordination structures is carried out at high temperature in order for the reaction to quickly reach an equilibrium. However, in the present work we conducted the self-assembly of the $[Pd_6L_8]^{12+}$ capsules at lower temperature of 298 K to accurately investigate the self-assembly process by ^{1}H NMR measurement.

58. If several kinds of fragmentary species exist after 25 min, the (n, k) value of the average composition of the fragmentary species, $(Pd_a1_bPy_c)_{ave}$, does not keep (2.87, 0.75) unless the rate of conversion of every fragmentary species is identical to each other, because the (n, k) is a function of the composition ratio of the fragmentary species. For example, when fragmentary species **B** (n_B, k_B) and **C** (n_C, k_C) exist in a $x : y$ ratio in the reaction mixture, the (n, k) is $((x·n_B + y·n_C)/(x + y), (x·k_B + y·k_C)/(x + y))$. The (n, k) keeps the same value only when the composition ratio of **B** and **C** does not change during the assembly, that is, the conversion of **B** and **C** to the assembled structure takes place at the same rate. Such a situation would be less probable.

59. F. Basolo and R. G. Pearson, *Mechanisms of inorganic reactions*, **1967**, Wiley, New York.

60. L. Canovese, L. Cattalini, P. Uguagliati and M. L. Tobe, *J. Chem. Soc. Dalton Trans.,* 1990, 867 – 872.

61. R. G. Pearson, H. Harold Sobel and J. Songstad, *J. Am. Chem. Soc.,* 1968, **90**, 319 – 326.

62. In order to accurately compare the self-assembly process of $[Pd_61_8]^{12+}$, deuterium atoms instead of hydrogen atoms were introduced in the panel molecule **2** because ^{1}H NMR spectrum of **2** exhibits a similar coupling pattern to the panel molecule **1**.

63. $[Pd_6L_8Py_2]^{12+}$ has nine structural isomers, in which the place of two Py molecules attached to Pd^{2+} ion(s) is different. All the structures are shown in Fig. S6.

64. Electron-donating ability of the methyl groups in **1** may affect the coordination strength of the ligand. In this case, the rates of both the consumption of **1** and the release of Py should be faster than those of **2** at the beginning of the self-assembly. However, at 5 min both the rates are similar to each other, while after 15 min the two rates for **1** become faster (Figs. 5A and 5C). These results indicate that the acceleration of the formation of $[Pd_61_8Py_1]^{12+}$ should arise from stronger chelate cooperativity.

65. M. Antonietti and S. Förster, *Adv. Mater.,* 2003, **15**, 1329 – 1333.

66. D. A. Roberts, A. M. Castilla, T. K. Ronson and J. R. Nitschke, *J. Am. Chem. Soc.* 2014, **136**, 8201 – 8204.

67. F. U. Hartl, A. Bracher and M. Hayer-Hartl, *Nature,* 2011, **475**, 324 – 332.

Chemical Science Accepted Manuscript